Measurement of the $\Lambda_b^0 \to \Lambda(1520)\mu^+\mu^-$ Differential Branching Fraction

R. Aaij *et al.*[*]
(LHCb Collaboration)

(Received 16 February 2023; accepted 11 August 2023; published 10 October 2023)

The branching fraction of the rare decay $\Lambda_b^0 \to \Lambda(1520)\mu^+\mu^-$ is measured for the first time, in the squared dimuon mass intervals q^2, excluding the J/ψ and $\psi(2S)$ regions. The data sample analyzed was collected by the LHCb experiment at center-of-mass energies of 7, 8, and 13 TeV, corresponding to a total integrated luminosity of 9 fb^{-1}. The result in the highest q^2 interval, $q^2 > 15.0$ GeV$^2/c^4$, where theoretical predictions have the smallest model dependence, agrees with the predictions.

DOI: 10.1103/PhysRevLett.131.151801

The standard model (SM) of particle physics provides at present the best description of fundamental particles and their interactions. However, it is unable to explain the dominance of matter over antimatter or the patterns of the interaction strengths of the elementary particles. Physics beyond the SM (BSM) is needed to address these limitations.

One way of searching for BSM physics is to study the flavor changing neutral-current transition $b \to s\ell^+\ell^-$, which proceeds through electroweak loop diagrams in the SM, while a sizeable contribution could be introduced by BSM physics [1–3]. Such decays have been studied in the B-meson sector by measuring branching fractions [4–7] and angular distributions [8–18] and testing lepton flavor universality [19–25]. Similar to B-meson decays, the study of b-baryon decays offers a multitude of observables that are analogous to those typically measured in B-meson decays, including charge-parity (CP) asymmetries. Owing to the half-integer spin, the b-baryon decays offer an even richer angular structure than the B-meson decays [26].

The differential branching fraction and angular observables of the $\Lambda_b^0 \to \Lambda\mu^+\mu^-$ decay were analyzed by the LHCb Collaboration [27], and the measured values can be described by recent theoretical calculations [28,29]. The $\Lambda_b^0 \to pK^-\mu^+\mu^-$ decay was first observed by the LHCb Collaboration [30], and a search for CP violation was performed. A test of lepton flavor universality in the decay $\Lambda_b^0 \to pK^-\ell^+\ell^-$ was carried out by the LHCb Collaboration [31], and the result was found to be consistent with SM predictions. In the aforementioned measurements, there are various contributions of excited Λ baryon resonances to the pK^- final state, among which the $\Lambda(1520)$ stands out as having a relatively narrow width of 16 MeV [32]. In contrast to the ground state Λ, which has a spin parity of $J^P = (1/2)^-$, the excited $\Lambda(1520)$ state has a spin parity of $J^P = (3/2)^-$, providing complementary information on potential new physics effects in the $b \to s\ell^+\ell^-$ transitions [33].

This Letter reports the first measurement of the differential branching fraction of the $\Lambda_b^0 \to \Lambda(1520)\mu^+\mu^-$ decay in intervals of the squared dimuon mass, q^2, with the $\Lambda(1520)$ baryon reconstructed through its $\Lambda(1520) \to pK^-$ decay. The inclusion of charge-conjugate processes is implied throughout this Letter. The more abundant tree-level decay $\Lambda_b^0 \to pK^-J/\psi$, with a well-measured branching fraction [34], is used for normalization. The measurements are performed using proton-proton (pp) collision data corresponding to an integrated luminosity of 9 fb^{-1} recorded by the LHCb experiment at center-of-mass energies of 7, 8, and 13 TeV.

The LHCb detector [35,36] is a single-arm forward spectrometer covering the pseudorapidity range $2 < \eta < 5$, designed for the study of particles containing b or c quarks. The online event selection is performed by a trigger [37,38], which consists of a hardware stage, based on information from the calorimeters and muon systems [39], followed by a software stage, which applies a full event reconstruction. Simulated events are used to develop the candidate selection and to estimate the corresponding efficiency for the signal and normalization modes. In the simulation, pp collisions are generated using PYTHIA 8 [40,41] with a specific LHCb configuration [42]. Decays of unstable particles are described by EvtGen [43], in which final-state radiation is generated using Photos [44]. The interaction of the generated particles with the detector, and its response, are simulated using the Geant4 toolkit [45] as described in Ref. [46]. The $\Lambda_b^0 \to \Lambda(1520)\mu^+\mu^-$ and $\Lambda_b^0 \to pK^-J/\psi$ decays are simulated following a uniform phase-space model. The intermediate resonant structures in the $\Lambda_b^0 \to pK^-J/\psi$ decay are

[*]Full author list given at the end of the Letter.

subsequently taken into account by using an unbinned approach with a correction based on the amplitude analysis in Ref. [47]. This approach takes into account both the two-body masses and the helicity angles. The Λ_b^0 lifetime in the simulation is corrected to its known value [34]. In addition, the detector occupancy and Λ_b^0 transverse momentum, $p_T(\Lambda_b^0)$, distributions of all simulated samples involving Λ_b^0 decays are corrected for discrepancies between the simulation and data, using $\Lambda_b^0 \to pK^-J/\psi$ samples.

Candidate $\Lambda(1520)$ baryon decays are reconstructed from two oppositely charged tracks identified as a proton and a kaon originating from a common vertex. No requirement on the $m(pK^-)$ mass is applied. The $\Lambda_b^0 \to \Lambda(1520)(\to pK^-)\mu^+\mu^-$ decay is reconstructed by combining a pK^- candidate with two oppositely charged tracks identified as muons. Dimuon pairs having mass squared q^2 values around the J/ψ ($8.0 < q^2 < 11.0\ \mathrm{GeV}^2/c^4$) and $\psi(2S)$ ($12.5 < q^2 < 15.0 < \mathrm{GeV}^2/c^4$) resonances are vetoed from the signal decay sample, while the candidates from the $\Lambda_b^0 \to pK^-J/\psi$ decay are used for normalization. The background is further suppressed by requirements on the quality of the Λ_b^0 decay vertex, the flight distance significance of the Λ_b^0 candidate, the compatibility of the Λ_b^0 candidate to come from the primary pp interaction vertex (PV), and the separation of the final-state tracks from the PV. For the $\Lambda_b^0 \to pK^-J/\psi$ decay, the mass of the Λ_b^0 candidate is recalculated with the J/ψ meson mass constrained to its known value [34], leading to an improvement on the Λ_b^0 mass resolution.

Various vetoes on hadron and muon masses reject peaking backgrounds originating from misidentified b-hadron decays, by recalculating the mass of the four-track combination under alternative particle hypotheses and removing candidates in the relevant mass range. Background candidates in the $\Lambda_b^0 \to \Lambda(1520)(\to pK^-)\mu^+\mu^-$ sample can originate from a few different sources. These include the $B_s^0 \to \phi(1020)(\to K^+K^-)\mu^+\mu^-$ decay, where a kaon is misidentified as a proton; contamination from $B^- \to K^-\mu^+\mu^-$ decays combined with a random additional proton; and the $\Lambda_b^0 \to pD^0(\to K^-\pi^+)\pi^-$ decay, where both pions are misidentified as muons. The same vetoes on the B_s^0 and B^- decays are used to reject backgrounds in the $\Lambda_b^0 \to pK^-J/\psi$ data sample. Owing to the narrow J/ψ mass window requirement, the $\Lambda_b^0 \to pD^0(\to K^-\pi^+)\pi^-$ background is negligible for the $\Lambda_b^0 \to pK^-J/\psi$ decay, and therefore the veto is not applied. The J/ψ contamination in the signal decay sample with a muon misidentified as a hadron is found to be negligible. These vetoes retain about 91% of the signal while strongly suppressing all these background sources. The background from $\Lambda_b^0 \to \Lambda_c^+(\to pK^-X)Y$ decays, where X and Y can represent either a $\mu^-\bar{\nu}_\mu(\mu^+\nu_\mu)$ pair or a pion, are verified to be negligible in the $\Lambda_b^0 \to \Lambda(1520)(\to pK^-)\mu^+\mu^-$ sample.

In order to increase the signal purity, a multivariate classification is employed using a boosted decision tree (BDT) [48,49] algorithm implemented in the TMVA package [50]. To train this classifier, simulated $\Lambda_b^0 \to \Lambda(1520)(\to pK^-)\mu^+\mu^-$ candidates are used as the signal proxy, and candidates lying in the upper $pK^-\ \mu^+\mu^-$ mass sideband (6.0–6.8 GeV/c^2) adjacent to the signal region are used as background proxy. The variables used in the BDT training include kinematical and topological properties of the final state or intermediate particles. The requirement on the multivariate output is optimized by maximizing the magnitude of $N_S/\sqrt{N_S+N_B}$, where N_S and N_B are the expected number of $\Lambda_b^0 \to \Lambda(1520)\mu^+\mu^-$ signal and background candidates underneath the signal peak, respectively. The BDT trained on the $\Lambda_b^0 \to \Lambda(1520)(\to pK^-)\mu^+\mu^-$ decay is also applied to the $\Lambda_b^0 \to pK^-J/\psi$ normalization mode, maintaining the same requirement on the multivariate output.

With the full selection applied, the differential branching fraction of the $\Lambda_b^0 \to \Lambda(1520)\mu^+\mu^-$ decay is determined in intervals of q^2, relative to the $\Lambda_b^0 \to pK^-J/\psi$ normalization mode, according to

$$\left\{\frac{d\mathcal{B}[\Lambda_b^0 \to \Lambda(1520)\mu^+\mu^-]}{dq^2}\right\}_{q^2_{\mathrm{min}}}^{q^2_{\mathrm{max}}} = \frac{1}{(q^2_{\mathrm{max}} - q^2_{\mathrm{min}})} \frac{\mathcal{B}(\Lambda_b^0 \to pK^-J/\psi)\mathcal{B}(J/\psi \to \mu^+\mu^-)}{\mathcal{B}[\Lambda(1520) \to pK^-]} \frac{N_{\Lambda(1520)\mu^+\mu^-}}{N_{pK^-J/\psi}} \frac{\varepsilon_{pK^-J/\psi}}{\varepsilon_{\Lambda(1520)\mu^+\mu^-}}, \quad (1)$$

where $N_{pK^-J/\psi}$ and $\varepsilon_{pK^-J/\psi}$ are the yields and efficiencies of the normalization mode, and $N_{\Lambda(1520)\mu^+\mu^-}$ and $\varepsilon_{\Lambda(1520)\mu^+\mu^-}$ indicate the corresponding parameters for the signal mode in the q^2_{min}–q^2_{max} interval. The branching fractions $\mathcal{B}(\Lambda_b^0 \to pK^-J/\psi)$, $\mathcal{B}(J/\psi \to \mu^+\mu^-)$, and $\mathcal{B}[\Lambda(1520) \to pK^-]$ are $(3.2 \pm 0.6) \times 10^{-4}$, $(5.961 \pm 0.033)\%$, and $(22.5 \pm 0.5)\%$, respectively [34].

To determine the geometrical acceptance and the efficiencies of the trigger, reconstruction, and particle identification (PID) requirements, we utilize the simulation and apply corrections based on unbiased control samples selected from real data. These corrections are applied to simulated samples of the signal and normalization modes to refine their accuracy. The PID efficiencies for each channel are calculated from calibration data samples of muons, proton, kaons, and pions [51], and are applied as per-candidate weights to the simulation. Similarly, the trigger efficiency is corrected by comparing the efficiency in data

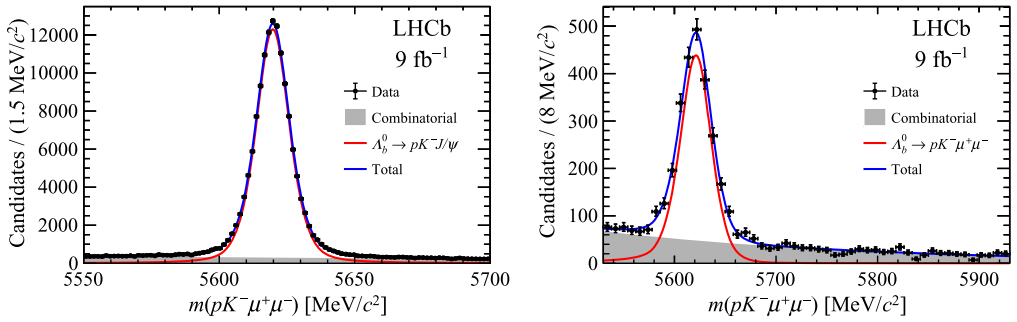

FIG. 1. Mass distribution for the (left) $\Lambda_b^0 \to pK^-J/\psi$ and (right) $\Lambda_b^0 \to pK^-\mu^+\mu^-$, integrated over the considered q^2 intervals. Fit results are overlaid.

and simulation as a function of the p_T of the muons in the normalization mode. Finally, the relative efficiencies for different data-taking periods are combined according to the integrated luminosity times the production rate of the Λ_b^0 baryon to account for the variation of data-taking conditions.

The yield of the $\Lambda_b^0 \to pK^-J/\psi$ normalization mode is determined using an extended unbinned maximum-likelihood fit to the pK^-J/ψ mass distribution with the J/ψ meson mass constrained to its known value [34]. The signal is modeled by a Hypatia function [52]. The tail parameters are determined from simulation, while the peak position and resolution are allowed to vary freely in the fit to data. The combinatorial background is modeled using an exponential function with the slope allowed to vary freely. The $m(pK^-\mu^+\mu^-)$ distribution of the selected $\Lambda_b^0 \to pK^-J/\psi$ candidates is shown in Fig. 1 (left), with the fit results overlaid. The $\Lambda_b^0 \to pK^-J/\psi$ yield is found to be $N_{pK^-J/\psi} = 137900 \pm 405$, where the uncertainty is statistical only.

For the $\Lambda_b^0 \to \Lambda(1520)\mu^+\mu^-$ decay, we perform a simultaneous extended unbinned maximum-likelihood fit to the $pK^-\mu^+\mu^-$ mass distribution in different intervals of q^2. The mean of the signal peak is shared among the different samples. The same signal and background models as for the $\Lambda_b^0 \to pK^-J/\psi$ normalization mode are used, while the tail parameters of the signal model are determined from the simulated $\Lambda_b^0 \to \Lambda(1520)\mu^+\mu^-$ sample. The $m(pK^-\mu^+\mu^-)$ resolution parameter for the signal component is fixed to the value obtained from a fit to the normalization mode. Figure 1 (right) shows the $m(pK^-\mu^+\mu^-)$ distribution of the full data sample, integrated over all the considered q^2 intervals. The $\Lambda_b^0 \to pK^-\mu^+\mu^-$ signal yield is found to be $N_{\Lambda_b^0 \to pK^-\mu^+\mu^-} = 2250 \pm 57$, where the uncertainty is statistical only. The corresponding figures for all the q^2 ranges are available as Supplemental Material [53].

The yields of the $\Lambda_b^0 \to \Lambda(1520)\mu^+\mu^-$ signal in the different q^2 bins are determined by maximizing the extended weighted log likelihood for unbinned $m(pK^-)$ distributions. The non-Λ_b^0 background is subtracted using the sPlot technique, which utilizes the $m(pK^-\mu^+\mu^-)$ distribution as a discriminating variable [54,55]. The efficiency as a function of $m(pK^-)$ is determined from simulation and included in the fit model. The fit procedure is validated with pseudoexperiments, and the uncertainties of the $\Lambda_b^0 \to \Lambda(1520)\mu^+\mu^-$ signal yields are corrected using the bootstrap method [56]. A cross-check is performed using unbinned maximum-likelihood fits to the two-dimensional $m(pK^-\mu^+\mu^-)$ and $m(pK^-)$ distributions, which give consistent results. Considering the mass and width of all the Λ states [34] and their contributions to the background-subtracted $m(pK^-)$ spectra, the $\Lambda(1405)$, $\Lambda(1520)$, $\Lambda(1600)$, and $\Lambda(1800)$ states are included in the nominal fits. The line shapes of these resonances are

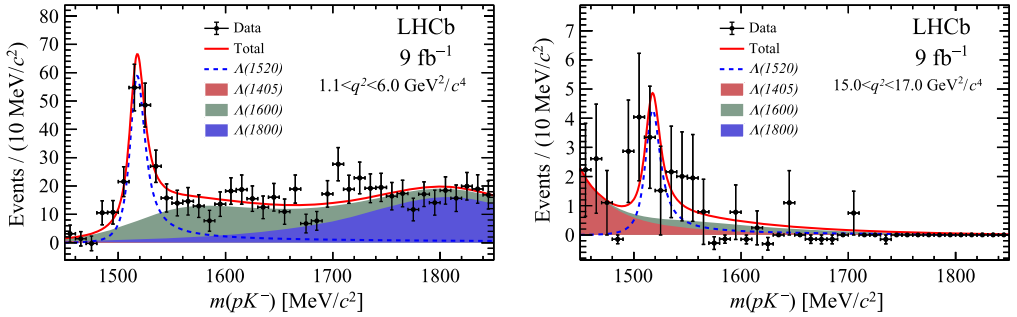

FIG. 2. Distribution of the pK^- mass, after background subtraction, for $\Lambda_b^0 \to pK^-\mu^+\mu^-$ signal candidates in the (left) $1.1 < q^2 < 6.0$ GeV$^2/c^4$ and (right) $15.0 < q^2 < 17.0$ GeV$^2/c^4$ regions. Fit results are overlaid.

TABLE I. Relative systematic uncertainties [in %] of the differential branching fraction ratio measurement. The total uncertainty is obtained as the quadratic sum of the individual contributions.

	q^2 interval (GeV^2/c^4)					
Source	0.1–3.0	3.0–6.0	6.0–8.0	11.0–12.5	15.0–17.0	1.1–6.0
Signal fit model	9.6	6.5	9.3	9.3	15.3	7.2
Normalization fit model	1.3	1.3	1.3	1.3	1.3	1.3
Hardware trigger	0.3	0.5	0.2	0.1	0.1	0.3
PID	2.4	2.4	1.6	7.0	16.0	2.4
Simulation corrections	0.1	0.1	0.1	0.1	0.1	0.1
Decay model	1.7	2.6	4.8	4.0	5.4	0.9
Simulated sample size	0.2	0.2	0.2	0.3	0.5	0.1
$\mathcal{B}(J/\psi \to \mu^+\mu^-)/\mathcal{B}[\Lambda(1520) \to pK^-]$	2.3	2.3	2.3	2.3	2.3	2.3
Quadratic sum	10.4	7.9	10.9	12.6	22.9	8.1
$\mathcal{B}(\Lambda_b^0 \to pK^-J/\psi)$	18.8	18.8	18.8	18.8	18.8	18.8

parametrized using relativistic Breit–Wigner functions. As the $\Lambda(1520)$ resonance has a width that is comparable to the experimental resolution, the line shape is convolved with a Gaussian resolution function. The width of the Gaussian is taken from the simulation. In the fits to the background-subtracted $m(pK^-)$ distributions, the width and mass of all the Λ resonances are fixed according to the world's best results [32,57]. The $\Lambda(1670)$, $\Lambda(1690)$, $\Lambda(1820)$, and $\Lambda(1830)$ states, and interference effects are not included in the fits as these are found to be small, and a systematic uncertainty is included in that of the signal fit mode. The background-subtracted $m(pK^-)$ distribution in the q^2 regions 1.1–6.0 GeV^2/c^4 and 15.0–17.0 GeV^2/c^4 are shown in Fig. 2. The signal yields in all the q^2 intervals are given in Table II.

The differential branching fraction measurement is affected by systematic uncertainties in the yield determination and the efficiency estimation. Table I lists these systematic uncertainties. The total uncertainty is determined from the sum of all contributions in quadrature. The largest uncertainty is related to the uncertainty on the measured mass and width of the Λ resonances that are fixed in the signal fit model, and is estimated using pseudoexperiments. Pseudodata samples are generated according to an alternative model in which the mass and width of the Λ resonances are varied within their uncertainty [32,57], and input values for the Blatt-Weisskopf barrier functions [58] of the Λ resonances are varied, then fitted with the default model.

The systematic uncertainty of the Λ_b^0 yield determination is evaluated using pseudoexperiments. For both the signal mode $\Lambda_b^0 \to \Lambda(1520)\mu^+\mu^-$ and the $\Lambda_b^0 \to pK^-J/\psi$ normalization mode, an alternative model is used where the signal is described by a double-sided crystal ball function [59] and the background by a second-order Chebyshev polynomial function [60]. Pseudosamples are generated using the alternative model and fitted with the default model, and the observed deviation is assigned as the systematic uncertainty. Peaking backgrounds that remain after the vetoes introduced in the selection are neglected in the fit for the determination of the $\Lambda_b^0 \to pK^-J/\psi$ yield. The main sources of systematic uncertainty are caused by contributions from the $B_s^0 \to K^+K^-J/\psi$ and $B^0 \to K^+\pi^-J/\psi$ decays.

The hardware-trigger efficiencies are measured in bins of muon p_T using the $\Lambda_b^0 \to pK^-J/\psi$ data sample. The effect of an alternative binning scheme on the efficiency ratio is taken as a systematic uncertainty. The PID efficiency is

TABLE II. Signal yields and the absolute differential branching fraction, in bins of q^2, for the $\Lambda_b^0 \to \Lambda(1520)\mu^+\mu^-$ decay. The first uncertainty is statistical, the second systematic, and the third due to the uncertainty on the $\Lambda_b^0 \to pK^-J/\psi$ and $J/\psi \to \mu^+\mu^-$ branching fractions.

q^2 interval (GeV^2/c^4)	$N_{\Lambda(1520)\mu^+\mu^-}$	$d\mathcal{B}[\Lambda_b^0 \to \Lambda(1520)\mu^+\mu^-]/dq^2$ (10^{-8} GeV^{-2} c^4)
0.1–3.0	96 ± 18	$1.89 \pm 0.35 \pm 0.19 \pm 0.36$
3.0–6.0	138 ± 18	$2.42 \pm 0.32 \pm 0.17 \pm 0.45$
6.0–8.0	65 ± 14	$1.58 \pm 0.36 \pm 0.16 \pm 0.30$
11.0–12.5	59 ± 14	$2.07 \pm 0.47 \pm 0.26 \pm 0.39$
15.0–17.0	12 ± 5	$0.57 \pm 0.24 \pm 0.13 \pm 0.11$
1.1–6.0	175 ± 21	$1.95 \pm 0.23 \pm 0.16 \pm 0.37$

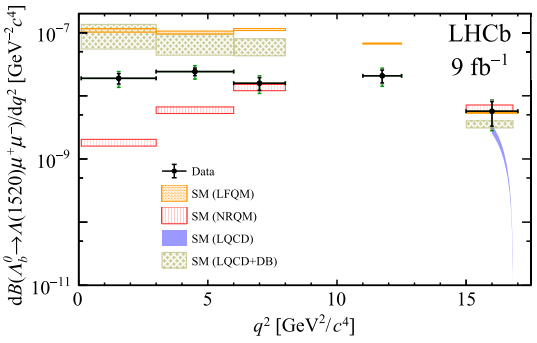

FIG. 3. Differential branching fraction of the $\Lambda_b^0 \to \Lambda(1520)\mu^+\mu^-$ decay in intervals of q^2. The error bars in black, gray, and green represent the measured results with statistical, systematic, and $\mathcal{B}(\Lambda_b^0 \to pK^-J/\psi)$ uncertainties taken into account. Also shown are the SM predictions using the form factors calculated with the nonrelativistic quark model (NRQM) [61], light-front quark model (LFQM) [62], joint lattice QCD and dispersive bound (LQCD + DB) [63] and lattice QCD (LQCD) [64]. Note that the LQCD prediction is only available for q^2 above 16 GeV$^2/c^4$, and the trend instead of a rate average is shown. These theoretical predictions as well as evaluation of the corresponding uncertainties should be revisited given their significant differences.

determined in bins of the particle momentum and pseudorapidity using calibration data samples. The effects of different binning schemes and different calibration samples are evaluated. The sum in quadrature of these effects is taken as the systematic uncertainty arising from the PID efficiency.

The systematic uncertainty associated with the simulation corrections is determined by using alternative binning schemes to account for the finite statistics of the control modes. The corresponding deviation is taken as the systematic uncertainty. The systematic uncertainty associated with the signal decay model used in simulation is estimated by taking the difference in efficiency between the phase-space model and the model given in Ref. [61]. In addition, the systematic uncertainties due to the limited size of the simulated sample and precision of the $J/\psi \to \mu^+\mu^-$ and $\Lambda(1520) \to pK^-$ branching fractions are also taken into account.

The differential branching fraction of the $\Lambda_b^0 \to \Lambda(1520)\mu^+\mu^-$ decay in intervals of q^2 is reported in Table II, and is shown in Fig. 3. The SM prediction from Ref. [61], for which only the form factor uncertainties are considered, and the SM prediction from Refs. [62] and [63], are also shown. It is impossible to make a firm statement about the level of agreement between the experimental measurement and the theoretical predictions due to the significant variation among the different theoretical predictions.

In summary, the first measurement of the branching fraction of the rare decay $\Lambda_b^0 \to \Lambda(1520)\mu^+\mu^-$ is presented using LHCb data corresponding to a total integrated luminosity of 9 fb^{-1}. The data are compared to several predictions within SM. In the highest q^2 interval, $q^2 > 15.0$ GeV$^2/c^4$, where the predictions have the smallest model dependence, they are consistent with the data. In the low-q^2 region, it is not possible to make a statement about the agreement between this experimental result and the predictions since the variation between the different SM predictions is much larger than their quoted uncertainties.

We express our gratitude to our colleagues in the CERN accelerator departments for the excellent performance of the LHC. We thank the technical and administrative staff at the LHCb institutes. We acknowledge support from CERN and from the national agencies: CAPES, CNPq, FAPERJ and FINEP (Brazil); MOST and NSFC (China); CNRS/IN2P3 (France); BMBF, DFG, and MPG (Germany); INFN (Italy); NWO (Netherlands); MNiSW and NCN (Poland); MCID/IFA (Romania); MICINN (Spain); SNSF and SER (Switzerland); NASU (Ukraine); STFC (United Kingdom); and DOE NP and NSF (USA). We acknowledge the computing resources that are provided by CERN, IN2P3 (France); KIT and DESY (Germany); INFN (Italy); SURF (Netherlands); PIC (Spain); GridPP (United Kingdom); CSCS (Switzerland); IFIN-HH (Romania); CBPF (Brazil); Polish WLCG (Poland); and NERSC (USA). We are indebted to the communities behind the multiple open-source software packages on which we depend. Individual groups or members have received support from ARC and ARDC (Australia); Minciencias (Colombia); AvH Foundation (Germany); EPLANET, Marie Skłodowska-Curie Actions, and ERC (European Union); A*MIDEX, ANR, IPhU and Labex P2IO, and Région Auvergne-Rhône-Alpes (France); Key Research Program of Frontier Sciences of CAS, CAS PIFI, CAS CCEPP, Fundamental Research Funds for the Central Universities, and Sci. & Tech. Program of Guangzhou (China); GVA, XuntaGal, GENCAT and Prog. Atracción Talento, CM (Spain); SRC (Sweden); the Leverhulme Trust, the Royal Society, and UKRI (United Kingdom).

[1] D. Das, Model independent new physics analysis in $\Lambda_b \to \Lambda\mu^+\mu^-$ decay, Eur. Phys. J. C **78**, 230 (2018).
[2] P. Langacker and M. Plumacher, Flavor changing effects in theories with a heavy Z' boson with family nonuniversal couplings, Phys. Rev. D **62**, 013006 (2000).
[3] S. Biswas, S. Mahata, B. P. Nayak, and S. Sahoo, Imprints of new physics in $\Lambda_b \to \Lambda^*\ell^+\ell^-$ decay in nonuniversal Z' model, Int. J. Mod. Phys. A **37**, 2250044 (2022).
[4] R. Aaij *et al.* (LHCb Collaboration), Measurement of the *CP* Asymmetry in $B^+ \to K^+\mu^+\mu^-$ Decays, Phys. Rev. Lett. **111**, 151801 (2013).
[5] R. Aaij *et al.* (LHCb Collaboration), Differential branching fractions and isospin asymmetries of $B \to K^{(*)}\mu^+\mu^-$ decays, J. High Energy Phys. 06 (2014) 133.

[6] R. Aaij *et al.* (LHCb Collaboration), Measurements of the S-wave fraction in $B^0 \to K^+\pi^-\mu^+\mu^-$ decays and the $B^0 \to K^*(892)^0\mu^+\mu^-$ differential branching fraction, J. High Energy Phys. 11 (2016) 047; 04 (2017) 142(E).

[7] R. Aaij *et al.* (LHCb Collaboration), Branching Fraction Measurements of the Rare $B_s^0 \to \phi\mu^+\mu^-$ and $B_s^0 \to f_2'(1525)\mu^+\mu^-$ Decays, Phys. Rev. Lett. **127**, 151801 (2021).

[8] T. Aaltonen *et al.* (CDF Collaboration), Measurements of the Angular Distributions in the Decays $B \to K^{(*)}\mu^+\mu^-$ at CDF, Phys. Rev. Lett. **108**, 081807 (2012).

[9] V. Khachatryan *et al.* (CMS Collaboration), Angular analysis of the decay $B^0 \to K^{*0}\mu^+\mu^-$ from pp collisions at $\sqrt{s} = 8$ TeV, Phys. Lett. B **753**, 424 (2016).

[10] A. M. Sirunyan *et al.* (CMS Collaboration), Measurement of angular parameters from the decay $B^0 \to K^{*0}\mu^+\mu^-$ in proton-proton collisions at $\sqrt{s} = 8$ TeV, Phys. Lett. B **781**, 517 (2018).

[11] A. M. Sirunyan *et al.* (CMS Collaboration), Angular analysis of the decay $B^+ \to K^+\mu^+\mu^-$ in proton-proton collisions at $\sqrt{s} = 8$ TeV, Phys. Rev. D **98**, 112011 (2018).

[12] M. Aaboud *et al.* (ATLAS Collaboration), Angular analysis of $B_d^0 \to K^*\mu^+\mu^-$ decays in pp collisions at $\sqrt{s} = 8$ TeV with the ATLAS detector, J. High Energy Phys. 10 (2018) 047.

[13] A. M. Sirunyan *et al.* (CMS Collaboration), Angular analysis of the decay $B^+ \to K^*(892)^+\mu^+\mu^-$ in proton-proton collisions at $\sqrt{s} = 8$ TeV, J. High Energy Phys. 04 (2021) 124.

[14] R. Aaij *et al.* (LHCb Collaboration), Angular analysis and differential branching fraction of the decay $B_s^0 \to \phi\mu^+\mu^-$, J. High Energy Phys. 09 (2015) 179.

[15] R. Aaij *et al.* (LHCb Collaboration), Angular analysis of the $B^0 \to K^{*0}\mu^+\mu^-$ decay using 3 fb^{-1} of integrated luminosity, J. High Energy Phys. 02 (2016) 104.

[16] S. Wehle *et al.* (Belle Collaboration), Lepton-Flavor-Dependent Angular Analysis of $B \to K^*\ell^+\ell^-$, Phys. Rev. Lett. **118**, 111801 (2017).

[17] R. Aaij *et al.* (LHCb Collaboration), Angular Analysis of the $B^+ \to K^{*+}\mu^+\mu^-$ Decay, Phys. Rev. Lett. **126**, 161802 (2021).

[18] R. Aaij *et al.* (LHCb Collaboration), Angular analysis of the rare decay $B_s^0 \to \phi\mu^+\mu^-$, J. High Energy Phys. 11 (2021) 043.

[19] J. P. Lees *et al.* (*BABAR* Collaboration), Measurement of branching fractions and rate asymmetries in the rare decays $B \to K^{(*)}\ell^+\ell^-$, Phys. Rev. D **86**, 032012 (2012).

[20] R. Aaij *et al.* (LHCb Collaboration), Search for Lepton-Universality Violation in $B^+ \to K^+\ell^+\ell^-$ Decays, Phys. Rev. Lett. **122**, 191801 (2019).

[21] S. Choudhury *et al.* (Belle Collaboration), Test of lepton flavor universality and search for lepton flavor violation in $B \to K\ell\ell$ decays, J. High Energy Phys. 03 (2021) 105.

[22] A. Abdesselam *et al.* (Belle Collaboration), Test of Lepton-Flavor Universality in $B \to K^*\ell^+\ell^-$ Decays at Belle, Phys. Rev. Lett. **126**, 161801 (2021).

[23] R. Aaij *et al.* (LHCb Collaboration), Tests of Lepton Universality Using $B^0 \to K_S^0\ell^+\ell^-$ and $B^+ \to K^{*+}\ell^+\ell^-$ Decays, Phys. Rev. Lett. **128**, 191802 (2022).

[24] R. Aaij *et al.* (LHCb Collaboration), Test of Lepton Universality in $b \to s\ell^+\ell^-$ Decays, Phys. Rev. Lett. **131**, 051803 (2023).

[25] R. Aaij *et al.* (LHCb Collaboration), Measurement of lepton universality parameters in $B^+ \to K^+\ell^+\ell^-$ and $B^0 \to K^{*0}\ell^+\ell^-$ decays, Phys. Rev. D **108**, 032002 (2023).

[26] T. Feldmann, Theory: Angular distributions in rare b decays, Proc. Sci., BEAUTY2020 (**2021**) 018.

[27] R. Aaij *et al.* (LHCb Collaboration), Differential branching fraction and angular analysis of $\Lambda_b^0 \to \Lambda\mu^+\mu^-$ decays, J. High Energy Phys. 06 (2015) 115; 09 (2018) 145(E).

[28] W. Detmold and S. Meinel, $\Lambda_b^0 \to \Lambda\ell^+\ell^-$ form factors, differential branching fraction, and angular observables from lattice QCD with relativistic b quarks, Phys. Rev. D **93**, 074501 (2016).

[29] T. Blake, S. Meinel, and D. van Dyk, Bayesian analysis of $b \to s\mu^+\mu^-$ Wilson coefficients using the full angular distribution of $\Lambda_b^0 \to \Lambda(\to p\pi^-)\mu^+\mu^-$ decays, Phys. Rev. D **101**, 035023 (2020).

[30] R. Aaij *et al.* (LHCb Collaboration), Observation of the decay $\Lambda_b^0 \to pK^-\mu^+\mu^-$ and search for CP violation, J. High Energy Phys. 06 (2017) 108.

[31] R. Aaij *et al.* (LHCb Collaboration), Test of lepton universality using $\Lambda_b^0 \to pK^-\ell^+\ell^-$ decays, J. High Energy Phys. 05 (2020) 040.

[32] A. V. Sarantsev, M. Matveev, V. A. Nikonov, A. V. Anisovich, U. Thoma, and E. Klempt, Hyperon II: Properties of excited hyperons, Eur. Phys. J. A **55**, 180 (2019).

[33] S. Meinel and G. Rendon, $\Lambda_b^0 \to \Lambda^*(1520)\ell^+\ell^-$ form factors from lattice QCD, Phys. Rev. D **103**, 074505 (2021).

[34] R. L. Workman *et al.* (Particle Data Group), Review of particle physics, Prog. Theor. Exp. Phys. **2022**, 083C01 (2022).

[35] A. A. Alves Jr. *et al.* (LHCb Collaboration), The LHCb detector at the LHC, J. Instrum. **3**, S08005 (2008).

[36] R. Aaij *et al.* (LHCb Collaboration), LHCb detector performance, Int. J. Mod. Phys. A **30**, 1530022 (2015).

[37] R. Aaij *et al.*, The LHCb trigger and its performance in 2011, J. Instrum. **8**, P04022 (2013).

[38] R. Aaij *et al.*, Design and performance of the LHCb trigger and full real-time reconstruction in Run 2 of the LHC, J. Instrum. **14**, P04013 (2019).

[39] F. Archilli *et al.*, Performance of the muon identification at LHCb, J. Instrum. **8**, P10020 (2013).

[40] T. Sjöstrand, S. Mrenna, and P. Skands, A brief introduction to PYTHIA 8.1, Comput. Phys. Commun. **178**, 852 (2008).

[41] T. Sjöstrand, S. Mrenna, and P. Skands, PYTHIA 6.4 physics and manual, J. High Energy Phys. 05 (2006) 026.

[42] I. Belyaev *et al.*, Handling of the generation of primary events in Gauss, the LHCb simulation framework, J. Phys. Conf. Ser. **331**, 032047 (2011).

[43] D. J. Lange, The EvtGen particle decay simulation package, Nucl. Instrum. Methods Phys. Res., Sect. A **462**, 152 (2001).

[44] P. Golonka and Z. Was, PHOTOS Monte Carlo: A precision tool for QED corrections in Z and W decays, Eur. Phys. J. C **45**, 97 (2006).

[45] J. Allison *et al.* (Geant4 Collaboration), Geant4 developments and applications, IEEE Trans. Nucl. Sci. **53**, 270

(2006); S. Agostinelli *et al.* (Geant4 Collaboration), Geant4: A simulation toolkit, Nucl. Instrum. Methods Phys. Res., Sect. A **506**, 250 (2003).
[46] M. Clemencic, G. Corti, S. Easo, C. R. Jones, S. Miglioranzi, M. Pappagallo, and P. Robbe, The LHCb simulation application, Gauss: Design, evolution and experience, J. Phys. Conf. Ser. **331**, 032023 (2011).
[47] R. Aaij *et al.* (LHCb Collaboration), Observation of $J/\psi p$ Resonances Consistent with Pentaquark States in $\Lambda_b^0 \to J/\psi p K^-$ Decays, Phys. Rev. Lett. **115**, 072001 (2015).
[48] L. Breiman, J. H. Friedman, R. A. Olshen, and C. J. Stone, *Classification and Regression Trees* (Wadsworth international group, Belmont, California, USA, 1984).
[49] B. P. Roe, H.-J. Yang, J. Zhu, Y. Liu, I. Stancu, and G. McGregor, Boosted decision trees, an alternative to artificial neural networks, Nucl. Instrum. Methods Phys. Res., Sect. A **543**, 577 (2005).
[50] H. Voss, A. Hoecker, J. Stelzer, and F. Tegenfeldt, TMVA—toolkit for multivariate data analysis with ROOT, Proc. Sci., ACAT2007 (**2007**) 040.
[51] R. Aaij *et al.*, Selection and processing of calibration samples to measure the particle identification performance of the LHCb experiment in Run 2, Eur. Phys. J. Tech. Instr. **6**, 1 (2019).
[52] D. Martínez Santos and F. Dupertuis, Mass distributions marginalized over per-event errors, Nucl. Instrum. Methods Phys. Res., Sect. A **764**, 150 (2014).
[53] See Supplemental Material at http://link.aps.org/supplemental/10.1103/PhysRevLett.131.151801 for the additional figures.
[54] M. Pivk and F. R. Le Diberder, sPlot: A statistical tool to unfold data distributions, Nucl. Instrum. Methods Phys. Res., Sect. A **555**, 356 (2005).
[55] Y. Xie, sFit: A method for background subtraction in maximum likelihood fit, arXiv:0905.0724.
[56] C. Langenbruch, Parameter uncertainties in weighted unbinned maximum likelihood fits, Eur. Phys. J. C **82**, 393 (2022).
[57] M. Hassanvand, S. Z. Kalantari, Y. Akaishi, and T. Yamazaki, Theoretical analysis of $\Lambda(1405) \to (\Sigma\pi)^0$ mass spectra produced in $p + p \to p + \Lambda(1405) + K^+$ reactions, Phys. Rev. C **87**, 055202 (2013); **88**, 019905(A) (2013).
[58] J. M. Blatt and V. F. Weisskopf, *Theoretical Nuclear Physics* (Springer, New York, 1952).
[59] T. Skwarnicki, A study of the radiative cascade transitions between the Upsilon-prime and Upsilon resonances, Ph.D. thesis, Institute of Nuclear Physics, Krakow, 1986, http://inspirehep.net/record/230779/.
[60] J. Smith, The chebyshev function: Theory and applications, Math. Rev. **42**, 135 (2010).
[61] S. Descotes-Genon and M. Novoa-Brunet, Angular analysis of the rare decay $\Lambda_b \to \Lambda(1520)(\to N\bar{K})\ell^+\ell^-$, J. High Energy Phys. 06 (2019) 136; 06 (2020) 102(E).
[62] Y.-S. Li, S.-P. Jin, J. Gao, and X. Liu, The angular analysis of $\Lambda_b \to \Lambda(1520)(\to N\bar{K})\ell^+\ell^-$ decay, Phys. Rev. D **107**, 093003 (2023).
[63] Y. Amhis, M. Bordone, and M. Reboud, Dispersive analysis of $\Lambda_b \to \Lambda(1520)$ local form factors, J. High Energy Phys. 02 (2023) 010.
[64] S. Meinel and G. Rendon, $\Lambda_c \to \Lambda^*(1520)$ form factors from lattice QCD and improved analysis of the $\Lambda_b \to \Lambda^*(1520)$ and $\Lambda_b \to \Lambda_c^*(2595, 2625)$ form factors, Phys. Rev. D **105**, 054511 (2022).

R. Aaij,[32] A. S. W. Abdelmotteleb,[50] C. Abellan Beteta,[44] F. Abudinén,[50] T. Ackernley,[54] B. Adeva,[40] M. Adinolfi,[48] P. Adlarson,[77] H. Afsharnia,[9] C. Agapopoulou,[13] C. A. Aidala,[78] Z. Ajaltouni,[9] S. Akar,[59] K. Akiba,[32] P. Albicocco,[23] J. Albrecht,[15] F. Alessio,[42] M. Alexander,[53] A. Alfonso Albero,[39] Z. Aliouche,[56] P. Alvarez Cartelle,[49] R. Amalric,[13] S. Amato,[2] J. L. Amey,[48] Y. Amhis,[11,42] L. An,[42] L. Anderlini,[22] M. Andersson,[44] A. Andreianov,[38] M. Andreotti,[21] D. Andreou,[62] D. Ao,[6] F. Archilli,[31,b] A. Artamonov,[38] M. Artuso,[62] E. Aslanides,[10] M. Atzeni,[44] B. Audurier,[79] I. Bachiller Perea,[8] S. Bachmann,[17] M. Bachmayer,[43] J. J. Back,[50] A. Bailly-reyre,[13] P. Baladron Rodriguez,[40] V. Balagura,[12] W. Baldini,[21,42] J. Baptista de Souza Leite,[1] M. Barbetti,[22,c] R. J. Barlow,[56] S. Barsuk,[11] W. Barter,[52] M. Bartolini,[49] F. Baryshnikov,[38] J. M. Basels,[14] G. Bassi,[29,d] B. Batsukh,[4] A. Battig,[15] A. Bay,[43] A. Beck,[50] M. Becker,[15] F. Bedeschi,[29] I. B. Bediaga,[1] A. Beiter,[62] S. Belin,[40] V. Bellee,[44] K. Belous,[38] I. Belov,[38] I. Belyaev,[38] G. Benane,[10] G. Bencivenni,[23] E. Ben-Haim,[13] A. Berezhnoy,[38] R. Bernet,[44] S. Bernet Andres,[76] D. Berninghoff,[17] H. C. Bernstein,[62] C. Bertella,[56] A. Bertolin,[28] C. Betancourt,[44] F. Betti,[42] Ia. Bezshyiko,[44] J. Bhom,[35] L. Bian,[68] M. S. Bieker,[15] N. V. Biesuz,[21] P. Billoir,[13] A. Biolchini,[32] M. Birch,[55] F. C. R. Bishop,[49] A. Bitadze,[56] A. Bizzeti, M. P. Blago,[49] T. Blake,[50] F. Blanc,[43] J. E. Blank,[15] S. Blusk,[62] D. Bobulska,[53] V. Bocharnikov,[38] J. A. Boelhauve,[15] O. Boente Garcia,[12] T. Boettcher,[59] A. Boldyrev,[38] C. S. Bolognani,[74] R. Bolzonella,[21,e] N. Bondar,[38,42] F. Borgato,[28] S. Borghi,[56] M. Borsato,[17] J. T. Borsuk,[35] S. A. Bouchiba,[43] T. J. V. Bowcock,[54] A. Boyer,[42] C. Bozzi,[21] M. J. Bradley,[55] S. Braun,[60] A. Brea Rodriguez,[40] N. Breer,[15] J. Brodzicka,[35] A. Brossa Gonzalo,[40] J. Brown,[54] D. Brundu,[27] A. Buonaura,[44] L. Buonincontri,[28] A. T. Burke,[56] C. Burr,[42] A. Bursche,[66] A. Butkevich,[38] J. S. Butter,[32] J. Buytaert,[42] W. Byczynski,[42] S. Cadeddu,[27] H. Cai,[68]

R. Calabrese,[21,e] L. Calefice,[15] S. Cali,[23] M. Calvi,[26,f] M. Calvo Gomez,[76] P. Campana,[23] D. H. Campora Perez,[74] A. F. Campoverde Quezada,[6] S. Capelli,[26,f] L. Capriotti,[20] A. Carbone,[20,g] R. Cardinale,[24,h] A. Cardini,[27] P. Carniti,[26,f] L. Carus,[14] A. Casais Vidal,[40] R. Caspary,[17] G. Casse,[54] M. Cattaneo,[42] G. Cavallero,[55,42] V. Cavallini,[21,e] S. Celani,[43] J. Cerasoli,[10] D. Cervenkov,[57] A. J. Chadwick,[54] I. Chahrour,[78] M. G. Chapman,[48] M. Charles,[13] Ph. Charpentier,[42] C. A. Chavez Barajas,[54] M. Chefdeville,[8] C. Chen,[10] S. Chen,[4] A. Chernov,[35] S. Chernyshenko,[46] V. Chobanova,[40] S. Cholak,[43] M. Chrzaszcz,[35] A. Chubykin,[38] V. Chulikov,[38] P. Ciambrone,[23] M. F. Cicala,[50] X. Cid Vidal,[40] G. Ciezarek,[42] P. Cifra,[42] P. E. L. Clarke,[52] M. Clemencic,[42] H. V. Cliff,[49] J. Closier,[42] J. L. Cobbledick,[56] V. Coco,[42] J. Cogan,[10] E. Cogneras,[9] L. Cojocariu,[37] P. Collins,[42] T. Colombo,[42] L. Congedo,[19] A. Contu,[27] N. Cooke,[47] I. Corredoira,[40] G. Corti,[42] B. Couturier,[42] D. C. Craik,[44] M. Cruz Torres,[1,i] R. Currie,[52] C. L. Da Silva,[61] S. Dadabaev,[38] L. Dai,[65] X. Dai,[5] E. Dall'Occo,[15] J. Dalseno,[40] C. D'Ambrosio,[42] J. Daniel,[9] A. Danilina,[38] P. d'Argent,[19] J. E. Davies,[56] A. Davis,[56] O. De Aguiar Francisco,[56] J. de Boer,[42] K. De Bruyn,[73] S. De Capua,[56] M. De Cian,[43] U. De Freitas Carneiro Da Graca,[1] E. De Lucia,[23] J. M. De Miranda,[1] L. De Paula,[2] M. De Serio,[19,j] D. De Simone,[44] P. De Simone,[23] F. De Vellis,[15] J. A. de Vries,[74] C. T. Dean,[61] F. Debernardis,[19,j] D. Decamp,[8] V. Dedu,[10] L. Del Buono,[13] B. Delaney,[58] H.-P. Dembinski,[15] V. Denysenko,[44] O. Deschamps,[9] F. Dettori,[27,k] B. Dey,[71] P. Di Nezza,[23] I. Diachkov,[38] S. Didenko,[38] L. Dieste Maronas,[40] S. Ding,[62] V. Dobishuk,[46] A. Dolmatov,[38] C. Dong,[3] A. M. Donohoe,[18] F. Dordei,[27] A. C. dos Reis,[1] L. Douglas,[53] A. G. Downes,[8] P. Duda,[75] M. W. Dudek,[35] L. Dufour,[42] V. Duk,[72] P. Durante,[42] M. M. Duras,[75] J. M. Durham,[61] D. Dutta,[56] A. Dziurda,[35] A. Dzyuba,[38] S. Easo,[51] U. Egede,[63] V. Egorychev,[38] C. Eirea Orro,[40] S. Eisenhardt,[52] E. Ejopu,[56] S. Ek-In,[43] L. Eklund,[77] M. Elashri,[59] J. Ellbracht,[15] S. Ely,[55] A. Ene,[37] E. Epple,[59] S. Escher,[14] J. Eschle,[44] S. Esen,[44] T. Evans,[56] F. Fabiano,[27,k] L. N. Falcao,[1] Y. Fan,[6] B. Fang,[11,68] L. Fantini,[72,l] M. Faria,[43] S. Farry,[54] D. Fazzini,[26,f] L. Felkowski,[75] M. Feo,[42] M. Fernandez Gomez,[40] A. D. Fernez,[60] F. Ferrari,[20] L. Ferreira Lopes,[43] F. Ferreira Rodrigues,[2] S. Ferreres Sole,[32] M. Ferrillo,[44] M. Ferro-Luzzi,[42] S. Filippov,[38] R. A. Fini,[19] M. Fiorini,[21,e] M. Firlej,[34] K. M. Fischer,[57] D. S. Fitzgerald,[78] C. Fitzpatrick,[56] T. Fiutowski,[34] F. Fleuret,[12] M. Fontana,[13] F. Fontanelli,[24,h] R. Forty,[42] D. Foulds-Holt,[49] V. Franco Lima,[54] M. Franco Sevilla,[60] M. Frank,[42] E. Franzoso,[21,e] G. Frau,[17] C. Frei,[42] D. A. Friday,[56] L. Frontini,[25,m] J. Fu,[6] Q. Fuehring,[15] T. Fulghesu,[13] E. Gabriel,[32] G. Galati,[19,j] M. D. Galati,[32] A. Gallas Torreira,[40] D. Galli,[20,g] S. Gambetta,[52,42] M. Gandelman,[2] P. Gandini,[25] H. Gao,[6] Y. Gao,[7] Y. Gao,[5] M. Garau,[27,k] L. M. Garcia Martin,[50] P. Garcia Moreno,[39] J. García Pardiñas,[42] B. Garcia Plana,[40] F. A. Garcia Rosales,[12] L. Garrido,[39] C. Gaspar,[42] R. E. Geertsema,[32] D. Gerick,[17] L. L. Gerken,[15] E. Gersabeck,[56] M. Gersabeck,[56] T. Gershon,[50] L. Giambastiani,[28] V. Gibson,[49] H. K. Giemza,[36] A. L. Gilman,[57] M. Giovannetti,[23] A. Gioventù,[40] P. Gironella Gironell,[39] C. Giugliano,[21,e] M. A. Giza,[35] K. Gizdov,[52] E. L. Gkougkousis,[42] V. V. Gligorov,[13,42] C. Göbel,[64] E. Golobardes,[76] D. Golubkov,[38] A. Golutvin,[55,38] A. Gomes,[1,1,2,a,n,o] S. Gomez Fernandez,[39] F. Goncalves Abrantes,[57] M. Goncerz,[35] G. Gong,[3] I. V. Gorelov,[38] C. Gotti,[26] J. P. Grabowski,[70] T. Grammatico,[13] L. A. Granado Cardoso,[42] E. Graugés,[39] E. Graverini,[43] G. Graziani, A. T. Grecu,[37] L. M. Greeven,[32] N. A. Grieser,[59] L. Grillo,[53] S. Gromov,[38] B. R. Gruberg Cazon,[57] C. Gu,[3] M. Guarise,[21,e] M. Guittiere,[11] P. A. Günther,[17] E. Gushchin,[38] A. Guth,[14] Y. Guz,[5,38,42] T. Gys,[42] T. Hadavizadeh,[63] C. Hadjivasiliou,[60] G. Haefeli,[43] C. Haen,[42] J. Haimberger,[42] S. C. Haines,[49] T. Halewood-leagas,[54] M. M. Halvorsen,[42] P. M. Hamilton,[60] J. Hammerich,[54] Q. Han,[7] X. Han,[17] S. Hansmann-Menzemer,[17] L. Hao,[6] N. Harnew,[57] T. Harrison,[54] C. Hasse,[42] M. Hatch,[42] J. He,[6,p] K. Heijhoff,[32] F. Hemmer,[42] C. Henderson,[59] R. D. L. Henderson,[63,50] A. M. Hennequin,[58] K. Hennessy,[54] L. Henry,[42] J. Herd,[55] J. Heuel,[14] A. Hicheur,[2] D. Hill,[43] M. Hilton,[56] S. E. Hollitt,[15] J. Horswill,[56] R. Hou,[7] Y. Hou,[8] J. Hu,[17] J. Hu,[66] W. Hu,[5] X. Hu,[3] W. Huang,[6] X. Huang,[68] W. Hulsbergen,[32] R. J. Hunter,[50] M. Hushchyn,[38] D. Hutchcroft,[54] P. Ibis,[15] M. Idzik,[34] D. Ilin,[38] P. Ilten,[59] A. Inglessi,[38] A. Iniukhin,[38] A. Ishteev,[38] K. Ivshin,[38] R. Jacobsson,[42] H. Jage,[14] S. J. Jaimes Elles,[41] S. Jakobsen,[42] E. Jans,[32] B. K. Jashal,[41] A. Jawahery,[60] V. Jevtic,[15] E. Jiang,[60] X. Jiang,[4,6] Y. Jiang,[6] M. John,[57] D. Johnson,[58] C. R. Jones,[49] T. P. Jones,[50] S. Joshi,[36] B. Jost,[42] N. Jurik,[42] I. Juszczak,[35] S. Kandybei,[45] Y. Kang,[3] M. Karacson,[42] D. Karpenkov,[38] M. Karpov,[38] J. W. Kautz,[59] F. Keizer,[42] D. M. Keller,[62] M. Kenzie,[50] T. Ketel,[32] B. Khanji,[15] A. Kharisova,[38] S. Kholodenko,[38] G. Khreich,[11] T. Kirn,[14] V. S. Kirsebom,[43]

O. Kitouni,[58] S. Klaver,[33] N. Kleijne,[29,d] K. Klimaszewski,[36] M. R. Kmiec,[36] S. Koliiev,[46] L. Kolk,[15] A. Kondybayeva,[38] A. Konoplyannikov,[38] P. Kopciewicz,[34] R. Kopecna,[17] P. Koppenburg,[32] M. Korolev,[38] I. Kostiuk,[32] O. Kot,[46] S. Kotriakhova, A. Kozachuk,[38] P. Kravchenko,[38] L. Kravchuk,[38] M. Kreps,[50] S. Kretzschmar,[14] P. Krokovny,[38] W. Krupa,[34] W. Krzemien,[36] J. Kubat,[17] S. Kubis,[75] W. Kucewicz,[35] M. Kucharczyk,[35] V. Kudryavtsev,[38] E. Kulikova,[38] A. Kupsc,[77] D. Lacarrere,[42] G. Lafferty,[56] A. Lai,[27] A. Lampis,[27,k] D. Lancierini,[44] C. Landesa Gomez,[40] J. J. Lane,[56] R. Lane,[48] C. Langenbruch,[14] J. Langer,[15] O. Lantwin,[38] T. Latham,[50] F. Lazzari,[29,q] C. Lazzeroni,[47] R. Le Gac,[10] S. H. Lee,[78] R. Lefèvre,[9] A. Leflat,[38] S. Legotin,[38] O. Leroy,[10] T. Lesiak,[35] B. Leverington,[17] A. Li,[3] H. Li,[66] K. Li,[7] P. Li,[42] P.-R. Li,[67] S. Li,[7] T. Li,[4] T. Li,[66] Y. Li,[4] Z. Li,[62] X. Liang,[62] C. Lin,[6] T. Lin,[51] R. Lindner,[42] V. Lisovskyi,[15] R. Litvinov,[27,k] G. Liu,[66] H. Liu,[6] K. Liu,[67] Q. Liu,[6] S. Liu,[4,6] A. Lobo Salvia,[39] A. Loi,[27] R. Lollini,[72] J. Lomba Castro,[40] I. Longstaff,[53] J. H. Lopes,[2] A. Lopez Huertas,[39] S. López Soliño,[40] G. H. Lovell,[49] Y. Lu,[4,r] C. Lucarelli,[22,c] D. Lucchesi,[28,s] S. Luchuk,[38] M. Lucio Martinez,[74] V. Lukashenko,[32,46] Y. Luo,[3] A. Lupato,[56] E. Luppi,[21,e] A. Lusiani,[29,d] K. Lynch,[18] X.-R. Lyu,[6] R. Ma,[6] S. Maccolini,[15] F. Machefert,[11] F. Maciuc,[37] I. Mackay,[57] V. Macko,[43] L. R. Madhan Mohan,[49] A. Maevskiy,[38] D. Maisuzenko,[38] M. W. Majewski,[34] J. J. Malczewski,[35] S. Malde,[57] B. Malecki,[35,42] A. Malinin,[38] T. Maltsev,[38] G. Manca,[27,k] G. Mancinelli,[10] C. Mancuso,[11,25,m] R. Manera Escalero,[39] D. Manuzzi,[20] C. A. Manzari,[44] D. Marangotto,[25,m] J. F. Marchand,[8] U. Marconi,[20] S. Mariani,[42] C. Marin Benito,[39] J. Marks,[17] A. M. Marshall,[48] P. J. Marshall,[54] G. Martelli,[72,l] G. Martellotti,[30] L. Martinazzoli,[42,f] M. Martinelli,[26,f] D. Martinez Santos,[40] F. Martinez Vidal,[41] A. Massafferri,[1] M. Materok,[14] R. Matev,[42] A. Mathad,[44] V. Matiunin,[38] C. Matteuzzi,[26] K. R. Mattioli,[12] A. Mauri,[55] E. Maurice,[12] J. Mauricio,[39] M. Mazurek,[42] M. McCann,[55] L. Mcconnell,[18] T. H. McGrath,[56] N. T. McHugh,[53] A. McNab,[56] R. McNulty,[18] B. Meadows,[59] G. Meier,[15] D. Melnychuk,[36] S. Meloni,[26,f] M. Merk,[32,74] A. Merli,[25,m] L. Meyer Garcia,[2] D. Miao,[4,6] H. Miao,[6] M. Mikhasenko,[70,t] D. A. Milanes,[69] E. Millard,[50] M. Milovanovic,[42] M.-N. Minard,[8,a] A. Minotti,[26,f] E. Minucci,[62] T. Miralles,[9] S. E. Mitchell,[52] B. Mitreska,[15] D. S. Mitzel,[15] A. Modak,[51] A. Mödden,[15] R. A. Mohammed,[57] R. D. Moise,[14] S. Mokhnenko,[38] T. Mombächer,[40] M. Monk,[50,63] I. A. Monroy,[69] S. Monteil,[9] G. Morello,[23] M. J. Morello,[29,d] M. P. Morgenthaler,[17] J. Moron,[34] A. B. Morris,[42] A. G. Morris,[10] R. Mountain,[62] H. Mu,[3] E. Muhammad,[50] F. Muheim,[52] M. Mulder,[73] K. Müller,[44] C. H. Murphy,[57] D. Murray,[56] R. Murta,[55] P. Muzzetto,[27,k] P. Naik,[48] T. Nakada,[43] R. Nandakumar,[51] T. Nanut,[42] I. Nasteva,[2] M. Needham,[52] N. Neri,[25,m] S. Neubert,[70] N. Neufeld,[42] P. Neustroev,[38] R. Newcombe,[55] J. Nicolini,[15,11] D. Nicotra,[74] E. M. Niel,[43] S. Nieswand,[14] N. Nikitin,[38] N. S. Nolte,[58] C. Normand,[8,27,k] J. Novoa Fernandez,[40] G. Nowak,[59] C. Nunez,[78] A. Oblakowska-Mucha,[34] V. Obraztsov,[38] T. Oeser,[14] S. Okamura,[21,e] R. Oldeman,[27,k] F. Oliva,[52] C. J. G. Onderwater,[73] R. H. O'Neil,[52] J. M. Otalora Goicochea,[2] T. Ovsiannikova,[38] P. Owen,[44] A. Oyanguren,[41] O. Ozcelik,[52] K. O. Padeken,[70] B. Pagare,[50] P. R. Pais,[42] T. Pajero,[57] A. Palano,[19] M. Palutan,[23] G. Panshin,[38] L. Paolucci,[50] A. Papanestis,[51] M. Pappagallo,[19,j] L. L. Pappalardo,[21,e] C. Pappenheimer,[59] W. Parker,[60] C. Parkes,[56,42] B. Passalacqua,[21,e] G. Passaleva,[22] A. Pastore,[19] M. Patel,[55] C. Patrignani,[20,g] C. J. Pawley,[74] A. Pellegrino,[32] M. Pepe Altarelli,[42] S. Perazzini,[20] D. Pereima,[38] A. Pereiro Castro,[40] P. Perret,[9] K. Petridis,[48] A. Petrolini,[24,h] S. Petrucci,[52] M. Petruzzo,[25] H. Pham,[62] A. Philippov,[38] R. Piandani,[6] L. Pica,[29,d] M. Piccini,[72] B. Pietrzyk,[8] G. Pietrzyk,[11] M. Pili,[57] D. Pinci,[30] F. Pisani,[42] M. Pizzichemi,[26,42,f] V. Placinta,[37] J. Plews,[47] M. Plo Casasus,[40] F. Polci,[13,42] M. Poli Lener,[23] A. Poluektov,[10] N. Polukhina,[38] I. Polyakov,[42] E. Polycarpo,[2] S. Ponce,[42] D. Popov,[6,42] S. Poslavskii,[38] K. Prasanth,[35] L. Promberger,[17] C. Prouve,[40] V. Pugatch,[46] V. Puill,[11] G. Punzi,[29,q] H. R. Qi,[3] W. Qian,[6] N. Qin,[3] S. Qu,[3] R. Quagliani,[43] N. V. Raab,[18] B. Rachwal,[34] J. H. Rademacker,[48] R. Rajagopalan,[62] M. Rama,[29] M. Ramos Pernas,[50] M. S. Rangel,[2] F. Ratnikov,[38] G. Raven,[33] M. Rebollo De Miguel,[41] F. Redi,[42] J. Reich,[48] F. Reiss,[56] C. Remon Alepuz,[41] Z. Ren,[3] P. K. Resmi,[57] R. Ribatti,[29,d] A. M. Ricci,[27] S. Ricciardi,[51] K. Richardson,[58] M. Richardson-Slipper,[52] K. Rinnert,[54] P. Robbe,[11] G. Robertson,[52] E. Rodrigues,[54,42] E. Rodriguez Fernandez,[40] J. A. Rodriguez Lopez,[69] E. Rodriguez Rodriguez,[40] D. L. Rolf,[42] A. Rollings,[57] P. Roloff,[42] V. Romanovskiy,[38] M. Romero Lamas,[40] A. Romero Vidal,[40] J. D. Roth,[78,a] M. Rotondo,[23] M. S. Rudolph,[62] T. Ruf,[42] R. A. Ruiz Fernandez,[40] J. Ruiz Vidal,[41] A. Ryzhikov,[38] J. Ryzka,[34] J. J. Saborido Silva,[40] N. Sagidova,[38] N. Sahoo,[47] B. Saitta,[27,k] M. Salomoni,[42] C. Sanchez Gras,[32] I. Sanderswood,[41] R. Santacesaria,[30] C. Santamarina Rios,[40] M. Santimaria,[23] L. Santoro,[1] E. Santovetti,[31,b]

D. Saranin,[38] G. Sarpis,[14] M. Sarpis,[70] A. Sarti,[30] C. Satriano,[30,u] A. Satta,[31] M. Saur,[15] D. Savrina,[38] H. Sazak,[9] L. G. Scantlebury Smead,[57] A. Scarabotto,[13] S. Schael,[14] S. Scherl,[54] A. M. Schertz,[71] M. Schiller,[53] H. Schindler,[42] M. Schmelling,[16] B. Schmidt,[42] S. Schmitt,[14] O. Schneider,[43] A. Schopper,[42] M. Schubiger,[32] N. Schulte,[15] S. Schulte,[43] M. H. Schune,[11] R. Schwemmer,[42] B. Sciascia,[23] A. Sciuccati,[42] S. Sellam,[40] A. Semennikov,[38] M. Senghi Soares,[33] A. Sergi,[24,h] N. Serra,[44] L. Sestini,[28] A. Seuthe,[15] Y. Shang,[5] D. M. Shangase,[78] M. Shapkin,[38] I. Shchemerov,[38] L. Shchutska,[43] T. Shears,[54] L. Shekhtman,[38] Z. Shen,[5] S. Sheng,[4,6] V. Shevchenko,[38] B. Shi,[6] E. B. Shields,[26,f] Y. Shimizu,[11] E. Shmanin,[38] R. Shorkin,[38] J. D. Shupperd,[62] B. G. Siddi,[21,e] R. Silva Coutinho,[62] G. Simi,[28] S. Simone,[19,j] M. Singla,[63] N. Skidmore,[56] R. Skuza,[17] T. Skwarnicki,[62] M. W. Slater,[47] J. C. Smallwood,[57] J. G. Smeaton,[49] E. Smith,[44] K. Smith,[61] M. Smith,[55] A. Snoch,[32] L. Soares Lavra,[9] M. D. Sokoloff,[59] F. J. P. Soler,[53] A. Solomin,[38,48] A. Solovev,[38] I. Solovyev,[38] R. Song,[63] F. L. Souza De Almeida,[2] B. Souza De Paula,[2] B. Spaan,[15,a] E. Spadaro Norella,[25,m] E. Spedicato,[20] J. G. Speer,[15] E. Spiridenkov,[38] P. Spradlin,[53] V. Sriskaran,[42] F. Stagni,[42] M. Stahl,[42] S. Stahl,[42] S. Stanislaus,[57] E. N. Stein,[42] O. Steinkamp,[44] O. Stenyakin,[38] H. Stevens,[15] D. Strekalina,[38] Y. Su,[6] F. Suljik,[57] J. Sun,[27] L. Sun,[68] Y. Sun,[60] P. N. Swallow,[47] K. Swientek,[34] A. Szabelski,[36] T. Szumlak,[34] M. Szymanski,[42] Y. Tan,[3] S. Taneja,[56] M. D. Tat,[57] A. Terentev,[44] F. Teubert,[42] E. Thomas,[42] D. J. D. Thompson,[47] H. Tilquin,[55] V. Tisserand,[9] S. T'Jampens,[8] M. Tobin,[4] L. Tomassetti,[21,e] G. Tonani,[25,m] X. Tong,[5] D. Torres Machado,[1] D. Y. Tou,[3] C. Trippl,[43] G. Tuci,[6] N. Tuning,[32] A. Ukleja,[36] D. J. Unverzagt,[17] A. Usachov,[33] A. Ustyuzhanin,[38] U. Uwer,[17] V. Vagnoni,[20] A. Valassi,[42] G. Valenti,[20] N. Valls Canudas,[76] M. Van Dijk,[43] H. Van Hecke,[61] E. van Herwijnen,[55] C. B. Van Hulse,[40,v] M. van Veghel,[32] R. Vazquez Gomez,[39] P. Vazquez Regueiro,[40] C. Vázquez Sierra,[42] S. Vecchi,[21] J. J. Velthuis,[48] M. Veltri,[22,w] A. Venkateswaran,[43] M. Veronesi,[32] M. Vesterinen,[50] D. Vieira,[59] M. Vieites Diaz,[43] X. Vilasis-Cardona,[76] E. Vilella Figueras,[54] A. Villa,[20] P. Vincent,[13] F. C. Volle,[11] D. vom Bruch,[10] V. Vorobyev,[38] N. Voropaev,[38] K. Vos,[74] C. Vrahas,[52] J. Walsh,[29] E. J. Walton,[63] G. Wan,[5] C. Wang,[17] G. Wang,[7] J. Wang,[5] J. Wang,[4] J. Wang,[3] J. Wang,[68] M. Wang,[25] R. Wang,[48] X. Wang,[66] Y. Wang,[7] Z. Wang,[44] Z. Wang,[3] Z. Wang,[6] J. A. Ward,[50,63] N. K. Watson,[47] D. Websdale,[55] Y. Wei,[5] B. D. C. Westhenry,[48] D. J. White,[56] M. Whitehead,[53] A. R. Wiederhold,[50] D. Wiedner,[15] G. Wilkinson,[57] M. K. Wilkinson,[59] I. Williams,[49] M. Williams,[58] M. R. J. Williams,[52] R. Williams,[49] F. F. Wilson,[51] W. Wislicki,[36] M. Witek,[35] L. Witola,[17] C. P. Wong,[61] G. Wormser,[11] S. A. Wotton,[49] H. Wu,[62] J. Wu,[7] K. Wyllie,[42] Z. Xiang,[6] Y. Xie,[7] A. Xu,[5] J. Xu,[6] L. Xu,[3] L. Xu,[3] M. Xu,[50] Q. Xu,[6] Z. Xu,[9] Z. Xu,[6] D. Yang,[3] S. Yang,[6] X. Yang,[5] Y. Yang,[6] Z. Yang,[5] Z. Yang,[60] L. E. Yeomans,[54] V. Yeroshenko,[11] H. Yeung,[56] H. Yin,[7] J. Yu,[65] X. Yuan,[62] E. Zaffaroni,[43] M. Zavertyaev,[16] M. Zdybal,[35] M. Zeng,[3] C. Zhang,[5] D. Zhang,[7] J. Zhang,[6] L. Zhang,[3] S. Zhang,[65] S. Zhang,[5] Y. Zhang,[5] Y. Zhang,[57] Y. Zhao,[17] A. Zharkova,[38] A. Zhelezov,[17] Y. Zheng,[6] T. Zhou,[5] X. Zhou,[7] Y. Zhou,[6] V. Zhovkovska,[11] X. Zhu,[3] X. Zhu,[7] Z. Zhu,[6] V. Zhukov,[14,38] Q. Zou,[4,6] S. Zucchelli,[20,g] D. Zuliani,[28] and G. Zunica[56]

(LHCb Collaboration)

[1]*Centro Brasileiro de Pesquisas Físicas (CBPF), Rio de Janeiro, Brazil*
[2]*Universidade Federal do Rio de Janeiro (UFRJ), Rio de Janeiro, Brazil*
[3]*Center for High Energy Physics, Tsinghua University, Beijing, China*
[4]*Institute Of High Energy Physics (IHEP), Beijing, China*
[5]*School of Physics State Key Laboratory of Nuclear Physics and Technology, Peking University, Beijing, China*
[6]*University of Chinese Academy of Sciences, Beijing, China*
[7]*Institute of Particle Physics, Central China Normal University, Wuhan, Hubei, China*
[8]*Université Savoie Mont Blanc, CNRS, IN2P3-LAPP, Annecy, France*
[9]*Université Clermont Auvergne, CNRS/IN2P3, LPC, Clermont-Ferrand, France*
[10]*Aix Marseille Univ, CNRS/IN2P3, CPPM, Marseille, France*
[11]*Université Paris-Saclay, CNRS/IN2P3, IJCLab, Orsay, France*
[12]*Laboratoire Leprince-Ringuet, CNRS/IN2P3, Ecole Polytechnique, Institut Polytechnique de Paris, Palaiseau, France*
[13]*LPNHE, Sorbonne Université, Paris Diderot Sorbonne Paris Cité, CNRS/IN2P3, Paris, France*
[14]*I. Physikalisches Institut, RWTH Aachen University, Aachen, Germany*

[15]Fakultät Physik, Technische Universität Dortmund, Dortmund, Germany
[16]Max-Planck-Institut für Kernphysik (MPIK), Heidelberg, Germany
[17]Physikalisches Institut, Ruprecht-Karls-Universität Heidelberg, Heidelberg, Germany
[18]School of Physics, University College Dublin, Dublin, Ireland
[19]INFN Sezione di Bari, Bari, Italy
[20]INFN Sezione di Bologna, Bologna, Italy
[21]INFN Sezione di Ferrara, Ferrara, Italy
[22]INFN Sezione di Firenze, Firenze, Italy
[23]INFN Laboratori Nazionali di Frascati, Frascati, Italy
[24]INFN Sezione di Genova, Genova, Italy
[25]INFN Sezione di Milano, Milano, Italy
[26]INFN Sezione di Milano-Bicocca, Milano, Italy
[27]INFN Sezione di Cagliari, Monserrato, Italy
[28]Università degli Studi di Padova, Università e INFN, Padova, Padova, Italy
[29]INFN Sezione di Pisa, Pisa, Italy
[30]INFN Sezione di Roma La Sapienza, Roma, Italy
[31]INFN Sezione di Roma Tor Vergata, Roma, Italy
[32]Nikhef National Institute for Subatomic Physics, Amsterdam, Netherlands
[33]Nikhef National Institute for Subatomic Physics and VU University Amsterdam, Amsterdam, Netherlands
[34]AGH - University of Science and Technology, Faculty of Physics and Applied Computer Science, Kraków, Poland
[35]Henryk Niewodniczanski Institute of Nuclear Physics Polish Academy of Sciences, Kraków, Poland
[36]National Center for Nuclear Research (NCBJ), Warsaw, Poland
[37]Horia Hulubei National Institute of Physics and Nuclear Engineering, Bucharest-Magurele, Romania
[38]Affiliated with an institute covered by a cooperation agreement with CERN
[39]ICCUB, Universitat de Barcelona, Barcelona, Spain
[40]Instituto Galego de Física de Altas Enerxías (IGFAE), Universidade de Santiago de Compostela, Santiago de Compostela, Spain
[41]Instituto de Fisica Corpuscular, Centro Mixto Universidad de Valencia - CSIC, Valencia, Spain
[42]European Organization for Nuclear Research (CERN), Geneva, Switzerland
[43]Institute of Physics, Ecole Polytechnique Fédérale de Lausanne (EPFL), Lausanne, Switzerland
[44]Physik-Institut, Universität Zürich, Zürich, Switzerland
[45]NSC Kharkiv Institute of Physics and Technology (NSC KIPT), Kharkiv, Ukraine
[46]Institute for Nuclear Research of the National Academy of Sciences (KINR), Kyiv, Ukraine
[47]University of Birmingham, Birmingham, United Kingdom
[48]H.H. Wills Physics Laboratory, University of Bristol, Bristol, United Kingdom
[49]Cavendish Laboratory, University of Cambridge, Cambridge, United Kingdom
[50]Department of Physics, University of Warwick, Coventry, United Kingdom
[51]STFC Rutherford Appleton Laboratory, Didcot, United Kingdom
[52]School of Physics and Astronomy, University of Edinburgh, Edinburgh, United Kingdom
[53]School of Physics and Astronomy, University of Glasgow, Glasgow, United Kingdom
[54]Oliver Lodge Laboratory, University of Liverpool, Liverpool, United Kingdom
[55]Imperial College London, London, United Kingdom
[56]Department of Physics and Astronomy, University of Manchester, Manchester, United Kingdom
[57]Department of Physics, University of Oxford, Oxford, United Kingdom
[58]Massachusetts Institute of Technology, Cambridge, Massachusetts, USA
[59]University of Cincinnati, Cincinnati, Ohio, USA
[60]University of Maryland, College Park, Maryland, USA
[61]Los Alamos National Laboratory (LANL), Los Alamos, New Mexico, USA
[62]Syracuse University, Syracuse, New York, USA
[63]School of Physics and Astronomy, Monash University, Melbourne, Australia
(associated with Department of Physics, University of Warwick, Coventry, United Kingdom)
[64]Pontifícia Universidade Católica do Rio de Janeiro (PUC-Rio), Rio de Janeiro, Brazil
(associated with Universidade Federal do Rio de Janeiro (UFRJ), Rio de Janeiro, Brazil)
[65]Physics and Micro Electronic College, Hunan University, Changsha City, China
(associated with Institute of Particle Physics, Central China Normal University, Wuhan, Hubei, China)
[66]Guangdong Provincial Key Laboratory of Nuclear Science, Guangdong-Hong Kong Joint Laboratory of Quantum Matter, Institute of Quantum Matter, South China Normal University, Guangzhou, China
(associated with Center for High Energy Physics, Tsinghua University, Beijing, China)
[67]Lanzhou University, Lanzhou, China
(associated with Institute Of High Energy Physics (IHEP), Beijing, China)

[68]School of Physics and Technology, Wuhan University, Wuhan, China
(associated with Center for High Energy Physics, Tsinghua University, Beijing, China)
[69]Departamento de Fisica, Universidad Nacional de Colombia, Bogota, Colombia
(associated with LPNHE, Sorbonne Université, Paris Diderot Sorbonne Paris Cité, CNRS/IN2P3, Paris, France)
[70]Universität Bonn - Helmholtz-Institut für Strahlen und Kernphysik, Bonn, Germany
(associated with Physikalisches Institut, Ruprecht-Karls-Universität Heidelberg, Heidelberg, Germany)
[71]Eotvos Lorand University, Budapest, Hungary
(associated with European Organization for Nuclear Research (CERN), Geneva, Switzerland)
[72]INFN Sezione di Perugia, Perugia, Italy
(associated with INFN Sezione di Ferrara, Ferrara, Italy)
[73]Van Swinderen Institute, University of Groningen, Groningen, Netherlands
(associated with Nikhef National Institute for Subatomic Physics, Amsterdam, Netherlands)
[74]Universiteit Maastricht, Maastricht, Netherlands
(associated with Nikhef National Institute for Subatomic Physics, Amsterdam, Netherlands)
[75]Tadeusz Kosciuszko Cracow University of Technology, Cracow, Poland
(associated with Henryk Niewodniczanski Institute of Nuclear Physics Polish Academy of Sciences, Kraków, Poland)
[76]DS4DS, La Salle, Universitat Ramon Llull, Barcelona, Spain
(associated with ICCUB, Universitat de Barcelona, Barcelona, Spain)
[77]Department of Physics and Astronomy, Uppsala University, Uppsala, Sweden
(associated with School of Physics and Astronomy, University of Glasgow, Glasgow, United Kingdom)
[78]University of Michigan, Ann Arbor, Michigan, USA
(associated with Syracuse University, Syracuse, New York, USA)
[79]Departement de Physique Nucleaire (SPhN), Gif-Sur-Yvette, France

[a]Deceased.
[b]Also at Università di Roma Tor Vergata, Roma, Italy.
[c]Also at Università di Firenze, Firenze, Italy.
[d]Also at Scuola Normale Superiore, Pisa, Italy.
[e]Also at Università di Ferrara, Ferrara, Italy.
[f]Also at Università di Milano Bicocca, Milano, Italy.
[g]Also at Università di Bologna, Bologna, Italy.
[h]Also at Università di Genova, Genova, Italy.
[i]Also at Universidad Nacional Autónoma de Honduras, Tegucigalpa, Honduras.
[j]Also at Università di Bari, Bari, Italy.
[k]Also at Università di Cagliari, Cagliari, Italy.
[l]Also at Università di Perugia, Perugia, Italy.
[m]Also at Università degli Studi di Milano, Milano, Italy.
[n]Also at Universidade Federal do Triângulo Mineiro (UFTM), Uberaba-MG, Brazil.
[o]Also at Universidade de Brasília, Brasília, Brazil.
[p]Also at Hangzhou Institute for Advanced Study, UCAS, Hangzhou, China.
[q]Also at Università di Pisa, Pisa, Italy.
[r]Also at Central South U., Changsha, China.
[s]Also at Università di Padova, Padova, Italy.
[t]Also at Excellence Cluster ORIGINS, Munich, Germany.
[u]Also at Università della Basilicata, Potenza, Italy.
[v]Also at Universidad de Alcalá, Alcalá de Henares, Spain.
[w]Also at Università di Urbino, Urbino, Italy.